

Supplementary online material

**Seasonal impact of biogenic VSL bromine on the evolution of mid-latitude lowermost stratospheric ozone during the 21<sup>st</sup> century**

Javier A. Barrera<sup>1</sup>, Rafael P. Fernandez<sup>1,2,3</sup>, Fernando Iglesias-Suarez<sup>2</sup>, Carlos A. Cuevas<sup>2</sup>, Jean-Francois Lamarque<sup>4</sup> and Alfonso Saiz-Lopez<sup>2</sup>

<sup>1</sup> Institute for Interdisciplinary Science, National Research Council (ICB-CONICET), FCEN-UNCuyo, Mendoza, 5500, Argentina.

<sup>2</sup> Department of Atmospheric Chemistry and Climate, Institute of Physical Chemistry Rocasolano, CSIC, Madrid, 28006, Spain.

<sup>3</sup> Atmospheric and Environmental Studies Group (GEAA), UTN-FRM, Mendoza, 5500, Argentina.

<sup>4</sup> Atmospheric Chemistry, Observations & Modelling Laboratory, National Center for Atmospheric Research, Boulder, CO 80301, USA

Table S1. Heterogeneous reactions on ice-crystals and sulphate aerosols involving halogens in CAM-Chem.

Reactions		Comments
Ice-crystal		
Het1	$\text{N}_2\text{O}_2 + \text{H}_2\text{O} \rightarrow 2\text{HNO}_3$	*
Het2	$\text{ClONO}_2 + \text{H}_2\text{O} \rightarrow \text{HOCl} + \text{HNO}_3$	*
Het3	$\text{BrONO}_2 + \text{H}_2\text{O} \rightarrow \text{HOBr} + \text{HNO}_3$	*
Het4	$\text{ClONO}_2 + \text{HCl} \rightarrow \text{Cl}_2 + \text{HNO}_3$	*
Het5	$\text{HOCl} + \text{HCl} \rightarrow \text{Cl}_2 + \text{H}_2\text{O}$	*
Het6	$\text{HOBr} + \text{HCl} \rightarrow \text{BrCl} + \text{H}_2\text{O}$	*
Sulfate aerosol reactions		
Het7	$\text{N}_2\text{O}_2 + \text{H}_2\text{O} \rightarrow 2\text{HNO}_3$	*
Het8	$\text{ClONO}_2 + \text{H}_2\text{O} \rightarrow \text{HOCl} + \text{HNO}_3$	*
Het9	$\text{BrONO}_2 + \text{H}_2\text{O} \rightarrow \text{HOBr} + \text{HNO}_3$	*
Het10	$\text{ClONO}_2 + \text{HCl} \rightarrow \text{Cl}_2 + \text{HNO}_3$	*
Het11	$\text{HOCl} + \text{HCl} \rightarrow \text{Cl}_2 + \text{H}_2\text{O}$	*
Het12	$\text{HOBr} + \text{HCl} \rightarrow \text{BrCl} + \text{H}_2\text{O}$	*

\* As in Table A4 from Auxiliary Material in Kinnison et al. (2007).

For a complete list of heterogeneous reactions implemented in CAM-Chem see Table 4 in the Supplementary Material of Ordoñez et al. (2012).

Table S2. Odd oxygen (Ox) loss rates reactions grouped by family cycles

Family	Reaction	$\Delta O_x$	Odd oxygen loss <sup>§</sup>
O <sub>x</sub>	$O + O_3 \rightarrow 2 \times O_2$	-2	$Ox_{-Loss} = 2 \times R_{O+O_3} + R_{O1D+H_2O}$
	$O(1D) + H_2O \rightarrow 2 \times OH$	-1	
HO <sub>x</sub>	$HO_2 + O \rightarrow OH + O_2$	-2 <sup>†</sup>	$HOx_{-Loss} = 2 \times (R_{HO_2+O} + R_{HO_2+O_3})$
	$HO_2 + O_3 \rightarrow OH + 2 \times O_2$	-2 <sup>†</sup>	
NO <sub>x</sub>	$NO_2 + O \rightarrow NO + O_2$	-2	$NOx_{-Loss} = 2 \times (R_{NO_2+O} + J_{NO_3})$
	$NO_3 + h\nu \rightarrow NO + O_2$	-2	
Halog	$ClO + O \rightarrow Cl + O_2$	-2	$ClOx_{-Loss} = 2 \times (R_{ClO+O} + J_{Cl_2O_2} + R_{ClO+ClO^a} + R_{ClO+ClO^b} + R_{ClO+HO_2})$
	$Cl_2O_2 + h\nu \rightarrow 2 \times Cl + O_2$	-2	
	$ClO + ClO \rightarrow Cl_2 + O_2$	-2	
	$ClO + ClO \rightarrow Cl + OClO$	-2	
	$ClO + HO_2 \rightarrow HOCl + O_2$	-2 <sup>‡</sup>	
	$BrO + O \rightarrow Br + O_2$	-2	$BrOx_{-Loss} = 2 \times (R_{BrO+O} + R_{BrO+BrO} + R_{BrO+HO_2})$
	$BrO + BrO \rightarrow 2 \times Br + O_2$	-2	
	$BrO + HO_2 \rightarrow HOBr + O_2$	-2 <sup>‡</sup>	
	$BrO + ClO \rightarrow Br + Cl + O_2$	-2	$ClOxBrOx_{-Loss} = 2 \times (R_{BrO+ClO^b} + R_{BrO+ClO^c})$
	$BrO + ClO \rightarrow BrCl + O_2$	-2	

$$O_x = O(3P) + O(1D) + O_3 + NO_2 + 2 \times NO_3 + HNO_3 + HO_2NO_2 + 2 \times N_2O_5 + ClO + 2 \times Cl_2O_2 + 2 \times OClO + 2 \times ClONO_2 + BrO + 2 \times BrONO_2$$

<sup>§</sup> $R_{A+B}$  is the reaction rate for reaction  $A+B \rightarrow \text{products}$  and  $J_C$  is the photodissociation rate constant (i.e. photolysis  $\times$  concentration) for  $C+h\nu \rightarrow \text{products}$ . Units are  $\text{molec.cm}^{-3}\text{s}^{-1}$ .

<sup>†</sup> $\text{HO}_x$  loss cycles represent a net change  $2\text{O}_3 \rightarrow 3\text{O}_2$  ( $\Delta\text{O}_x = -2$ ) due to reactions  $\text{OH} + \text{O} \rightarrow \text{H} + \text{O}_2$  and  $\text{OH} + \text{O}_3 \rightarrow \text{HO}_2 + \text{O}_2$ . As  $\text{O}_x$  reactions with OH are faster than with  $\text{HO}_2$ , only the rate determining steps (RDS) have been considered multiplied by two.

<sup>‡</sup>Reactions  $\text{XO} + \text{HO}_2 \rightarrow \text{HOX} + \text{O}_2$ , with  $\text{X} = \text{Cl}$  or  $\text{Br}$ , have been computed for each family with  $\Delta\text{O}_x = -2$  because the photolysis of HOX produces an additional  $\text{O}_x$  loss by the OH radical (i.e.  $\text{OH} + \text{O}_3 \rightarrow \text{HO}_2 + \text{O}_2$ ). As these  $\text{XO} + \text{HO}_2$  reaction are the rate limiting step, their loss rates have been multiplied by two.

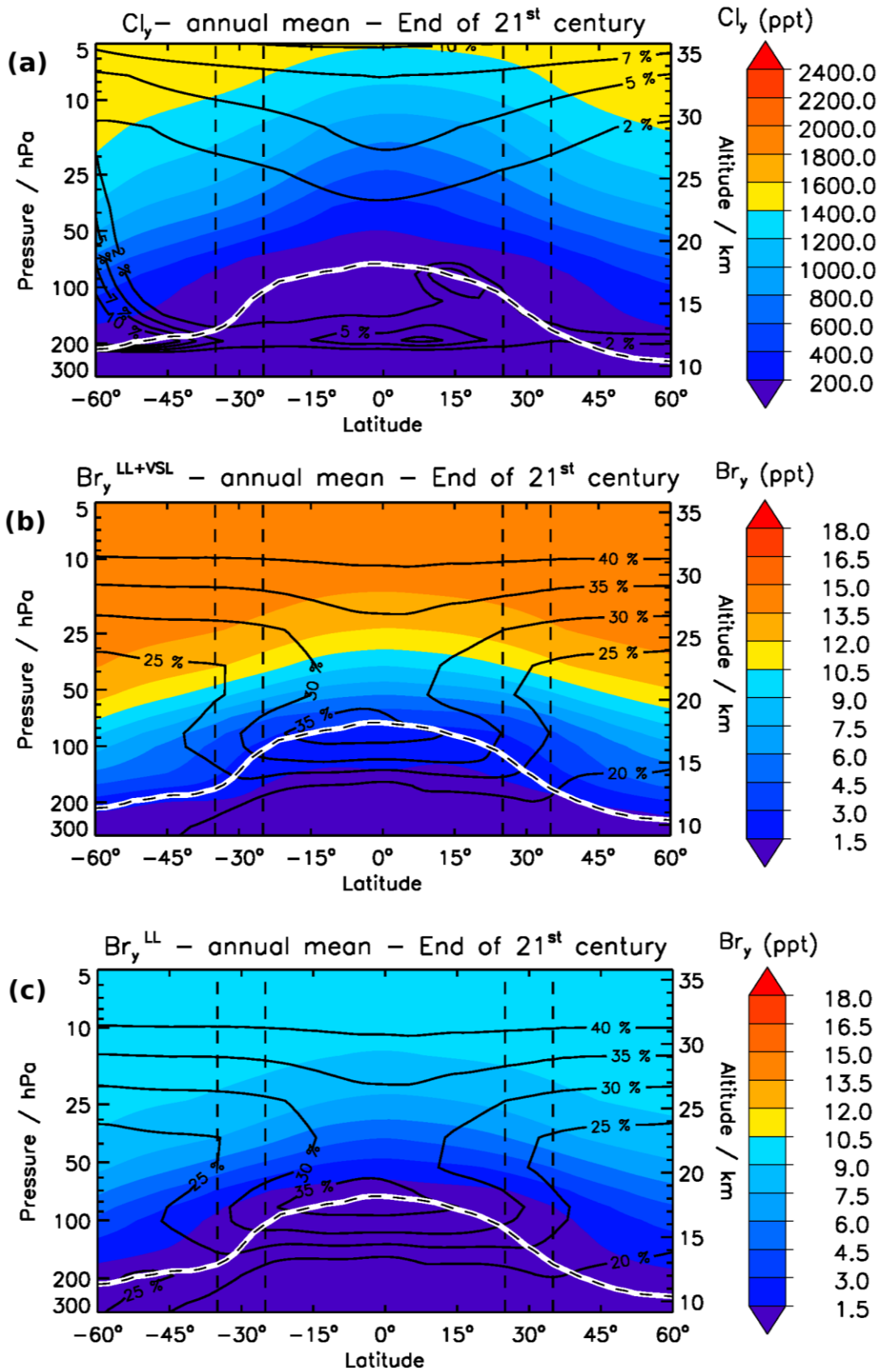


Figure S1: As Fig. 2 but for the end of the 21<sup>st</sup> century period.

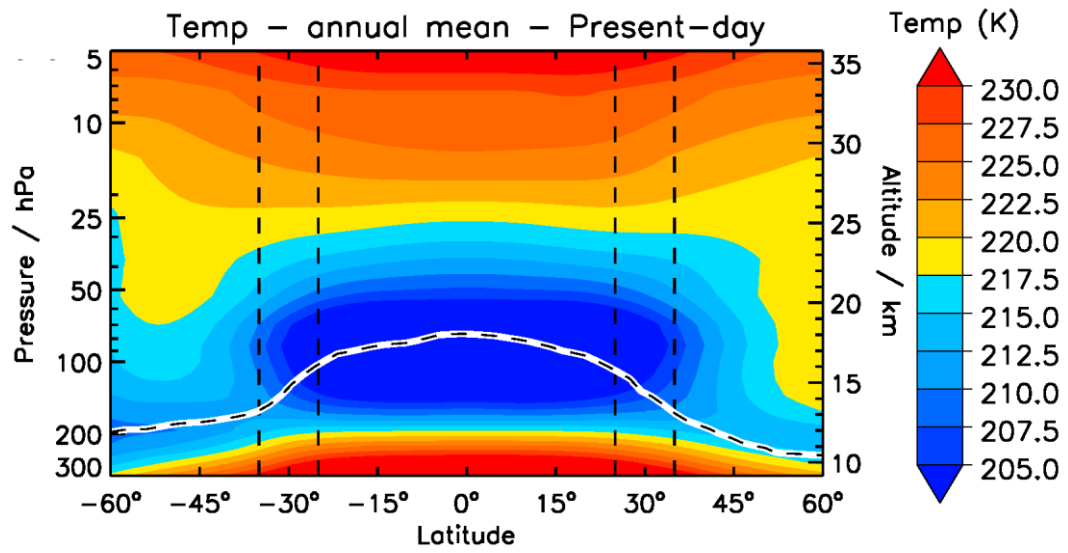
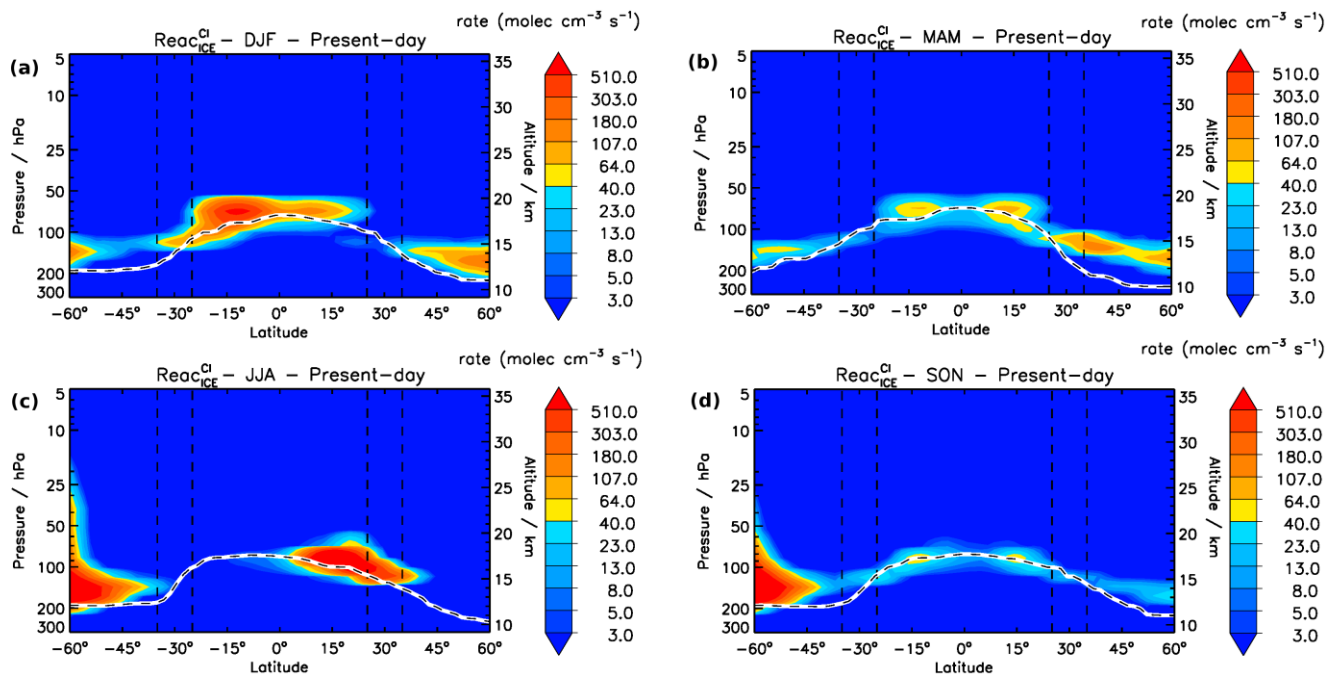


Figure S2: Annual zonal mean Temperature (K) for the present-day period. The lower solid white line indicates the location of the tropopause (chemical definition of 150 ppb ozone level from run<sup>LL</sup> experiments).



**Figure S3: Seasonal zonal mean distribution of the heterogeneous reactivation of  $\text{ClONO}_2$  (Het2,4) and  $\text{HOCl}$  (Het5) on ice-crystal during the present-day period. The reactions have been specified in table S1 with the label Het and the corresponding number.**

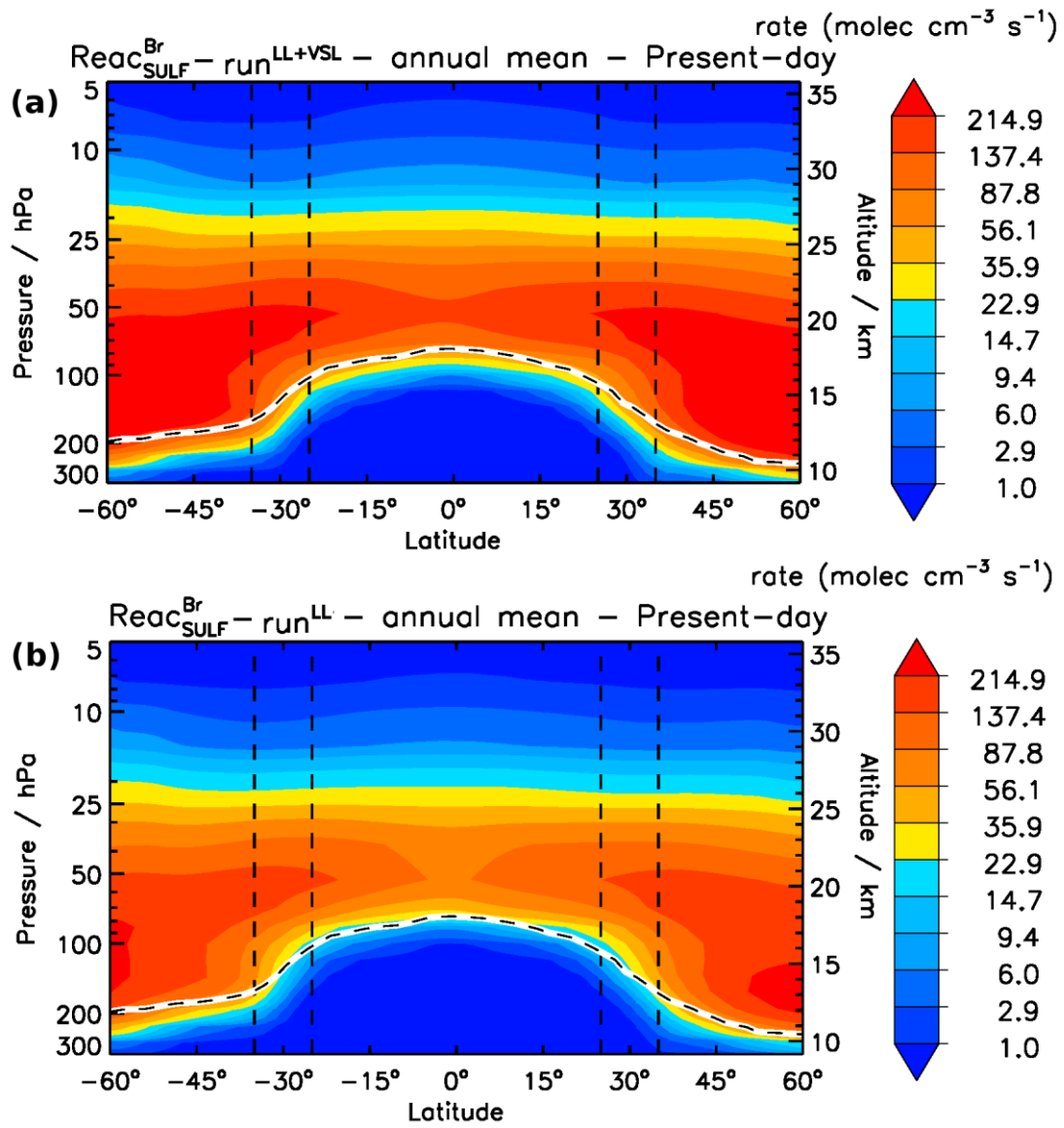


Figure S4: Annual zonal mean distribution of the heterogeneous reactivation of  $\text{BrONO}_2$  (Het9) and  $\text{HOBr}$  (Het12) on sulphate aerosols for the  $\text{run}^{\text{LL+vSL}}$  (a) and  $\text{run}^{\text{LL}}$  (b) experiments during the present-day period. The reactions have been specified in table S1 with the label Het and the corresponding number.



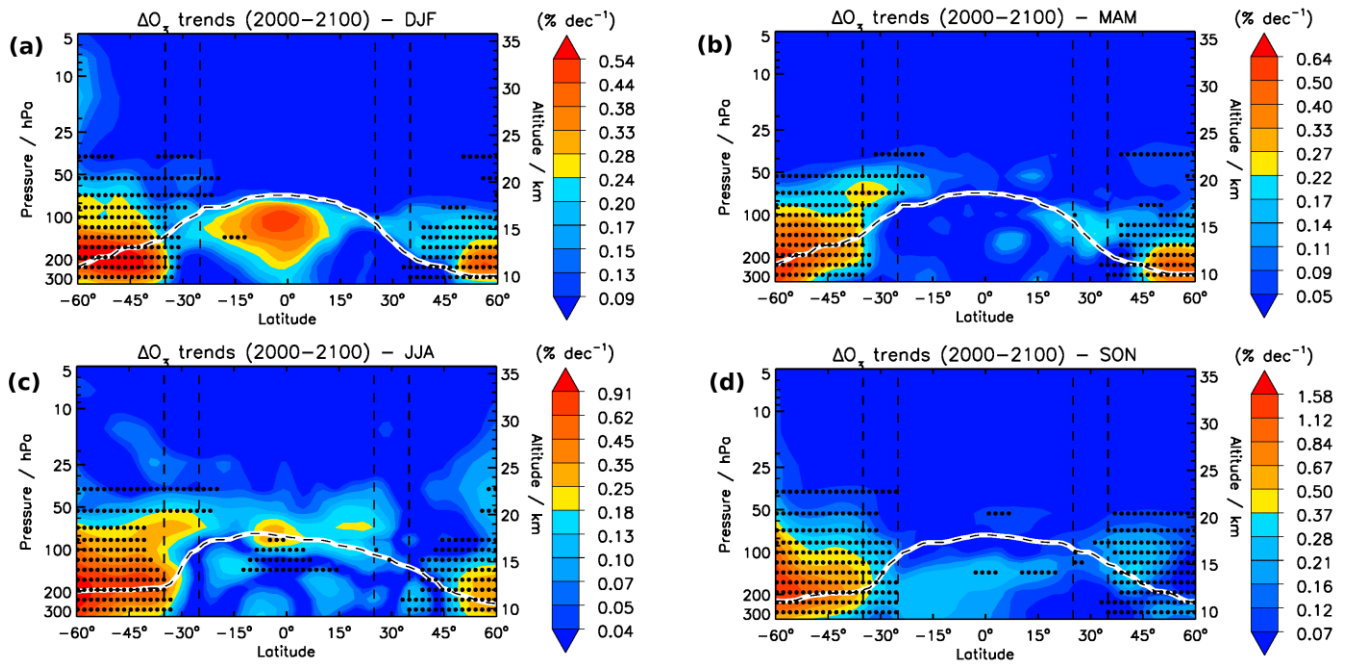


Figure S5: Zonal mean distributions of the seasonal  $\Delta O_3(z)$  trends ( $\% \text{ dec}^{-1}$ ) over the century. The masked regions in the left panels indicate where of seasonal relative  $\Delta O_3(z)$  between the present-day and the end of the 21<sup>st</sup> century periods are statistically significant at the 95% confidence interval using a two-tailed Student's  $t$  test.

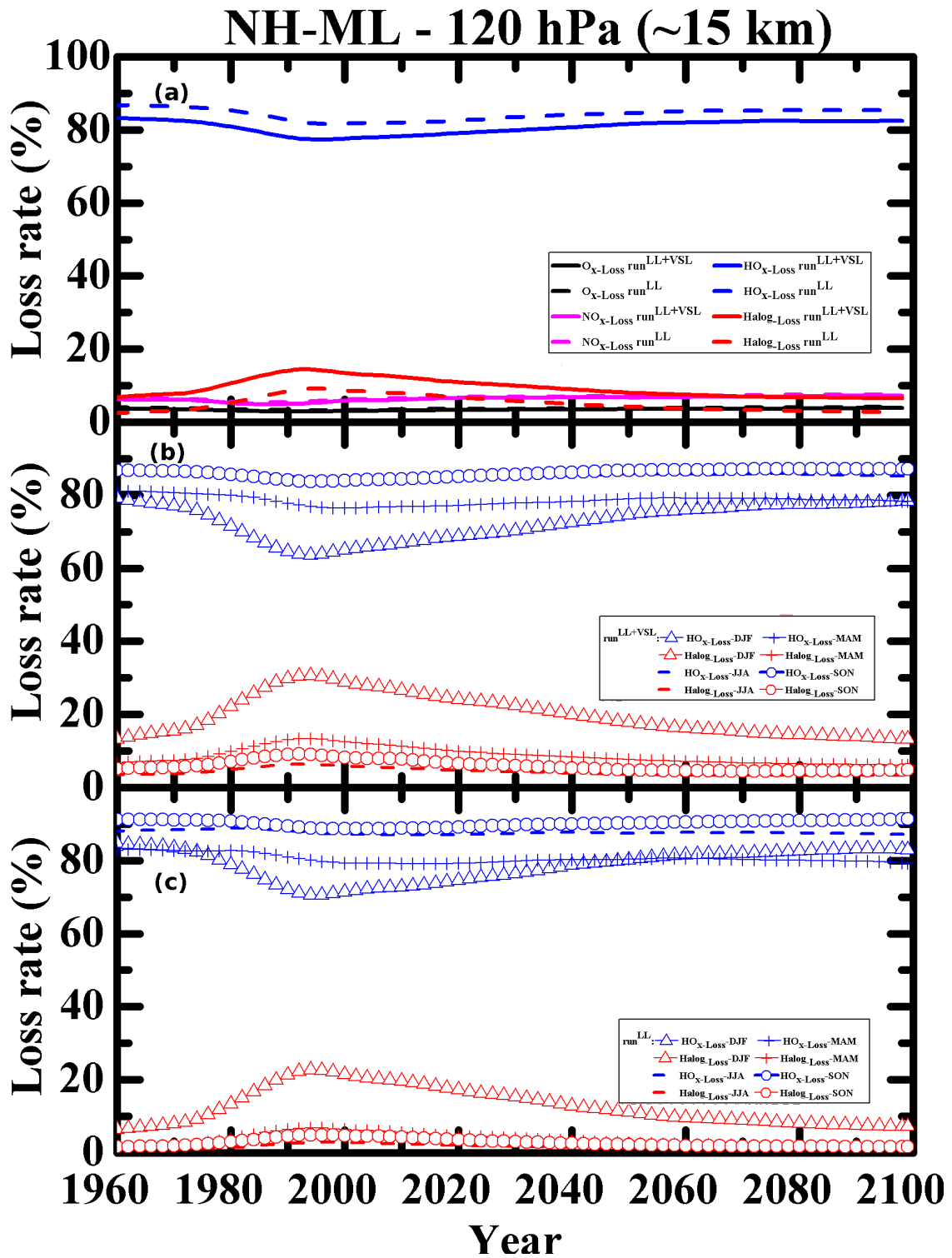


Figure S6: As Fig. 8 but for the lowermost stratosphere (120 hPa) at northern hemisphere mid-latitudes (NH-ML).

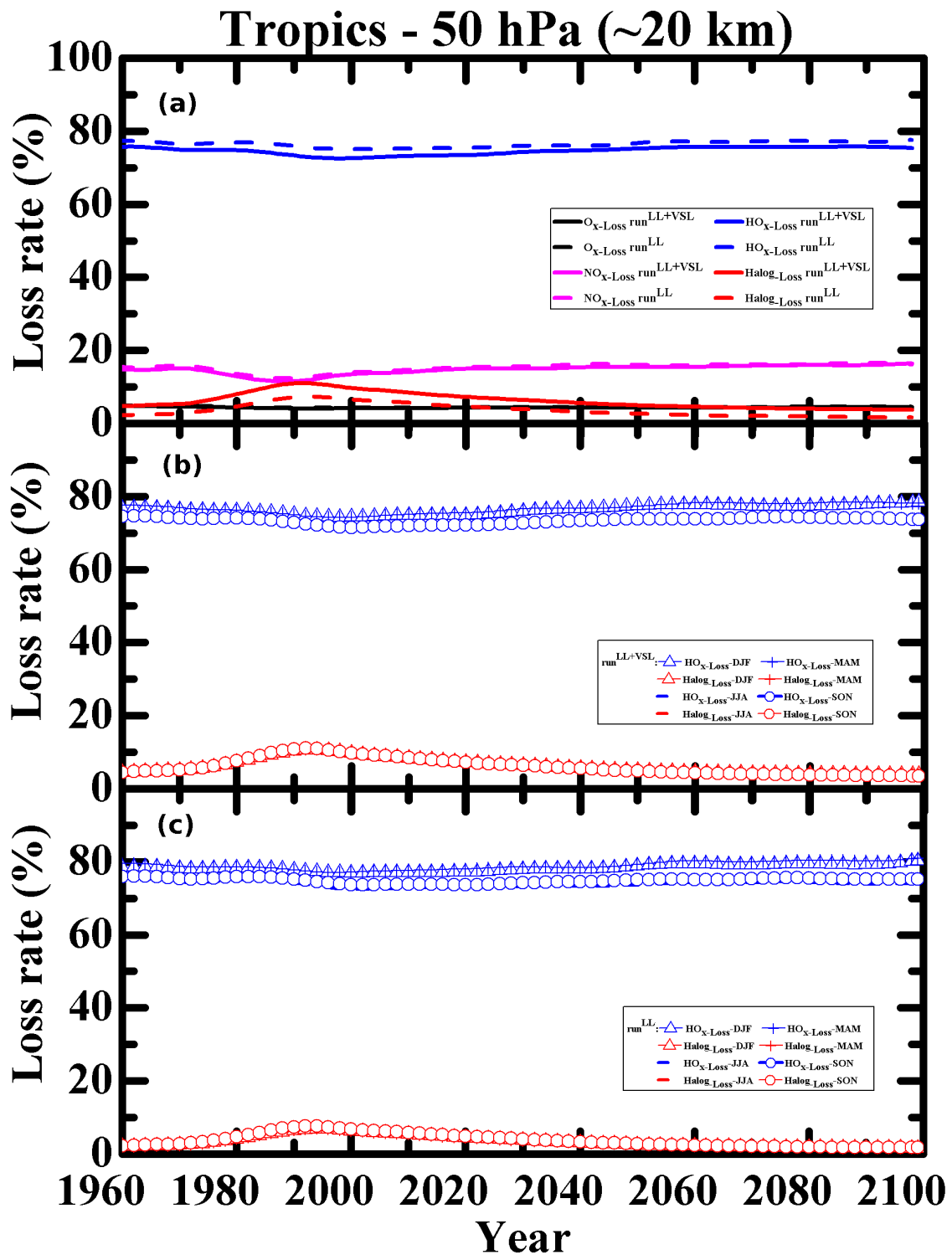


Figure S7: As Fig. 8 but for the lower stratosphere (50 hPa) at tropics.

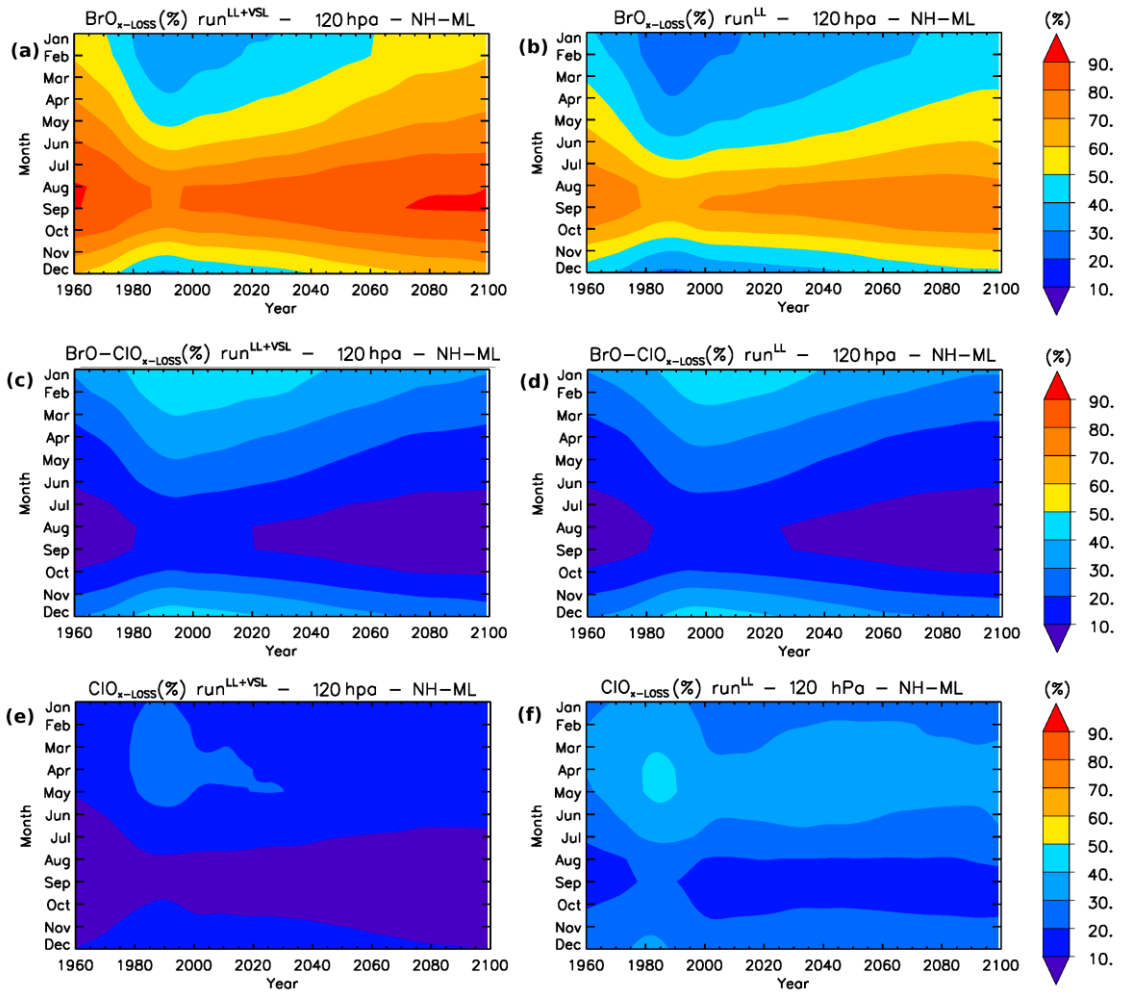


Figure S8: As Fig. 9 but for the lowermost stratosphere (120 hPa) at northern hemisphere mid-latitudes (NH-ML).

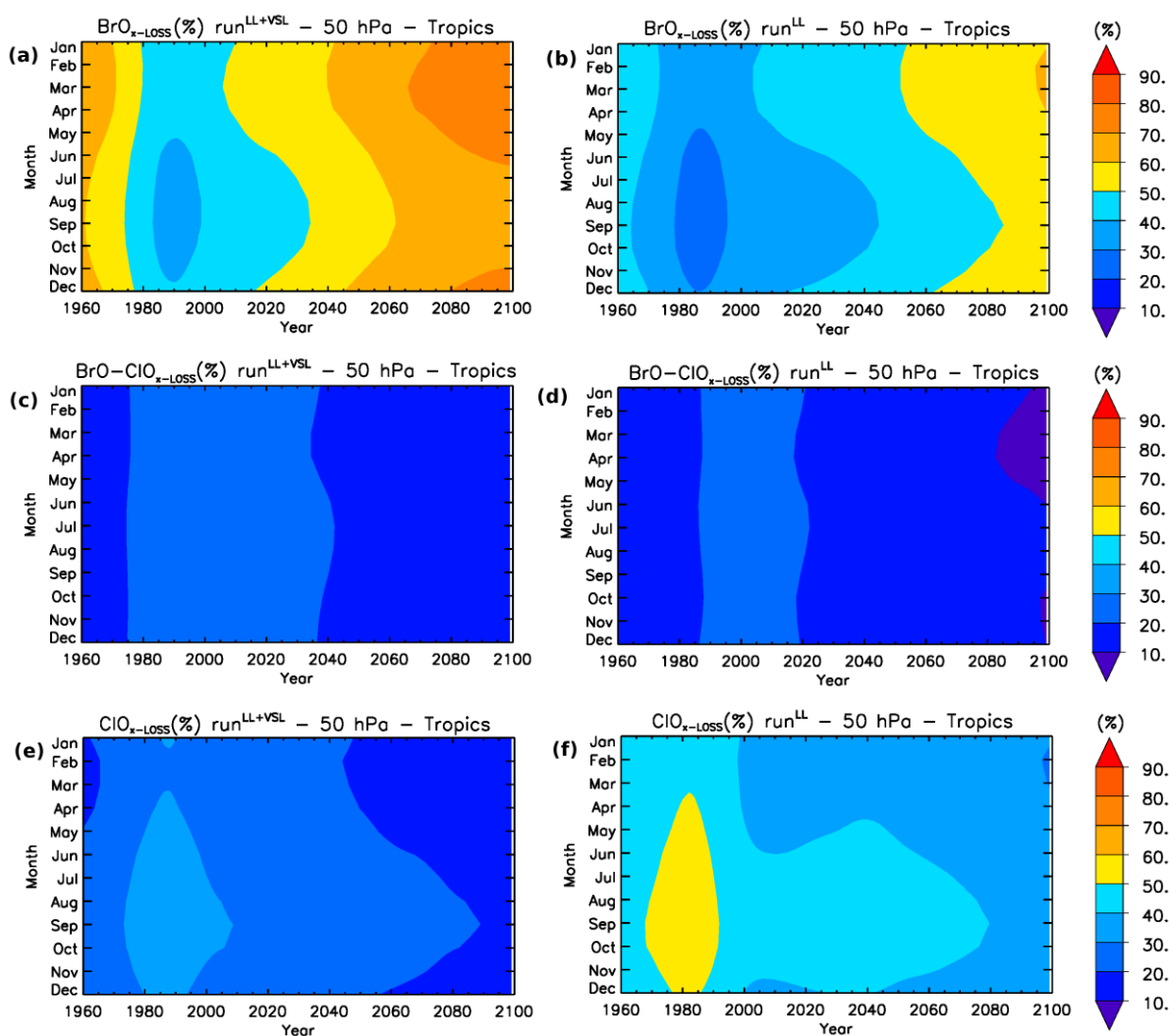


Figure S9: As Fig. 9 but for the lower stratosphere (50 hPa) at tropics.

## References

- Kinnison, D. E., Brasseur, G. P., Walters, S., Garcia, R. R., Marsh, D. R., and Sassi, F., Harvey, V. L., Randall, C. E., Emmons, L., Lamarque, J. F., Hess, P., Orlando, J. J., Tie, X. X., Randel, W., Pan, L. L., Gettelman, A., Granier, C., Diehl, T., Niemeier, U., and Simmons, A. J.: Sensitivity of chemical tracers to meteorological parameters in the MOZART-3 chemical transport model, *J. Geophys. Res.* 112, D20302, doi:10.1029/2006JD007879, 2007.
- Ordóñez, C., Lamarque, J.-F., Tilmes, S., Kinnison, D. E., Atlas, E. L., Blake, D. R., Sousa Santos, G., Brasseur, G. and Saiz-Lopez, A.: Bromine and iodine chemistry in a global chemistry-climate model: description and evaluation of very short-lived oceanic sources, *Atmos. Chem. Phys.*, 12, 1423–1447, <https://doi.org/10.5194/acp-12-1423-2012>, 2012.